AFRL-RX-WP-TP-2009-4162

INFLUENCE OF RESIDUAL STRESSES ON FRETTING FATIGUE LIFE PREDICTION IN Ti-6Al-4V (PREPRINT)

Patrick J. Golden, Dennis Buchanan and Sam Naboulsi

Metals Branch
Metals, Ceramics and NDE Division

JANUARY 2008

AIR FORCE RESEARCH LABORATORY
MATERIALS AND MANUFACTURING DIRECTORATE
WRIGHT-PATTERSON AIR FORCE BASE, OH 45433-7750
AIR FORCE MATERIEL COMMAND
UNITED STATES AIR FORCE

REPORT DOCUMENTATION PAGE

Form Approved
OMB No. 0704-0188

1. REPORT DATE *(DD-MM-YY)*	2. REPORT TYPE	3. DATES COVERED *(From - To)*
January 2008	Journal Article Preprint	01 January 2008 – 01 January 2008

4. TITLE AND SUBTITLE
INFLUENCE OF RESIDFUAL STRESSES ON FRETTING FATIGUE LIFE PREDICTION IN Ti-6Al-4V (PREPRINT)

5a. CONTRACT NUMBER
In-house

5b. GRANT NUMBER

5c. PROGRAM ELEMENT NUMBER
62102F

6. AUTHOR(S)
Patrick J. Golden (AFRL/RXLMN)
Dennis Buchanan (Dayton Research Institute)
Sam Naboulsi (The University of Texas)

5d. PROJECT NUMBER
4347

5e. TASK NUMBER
RG

5f. WORK UNIT NUMBER
M02R3000

7. PERFORMING ORGANIZATION NAME(S) AND ADDRESS(ES)

Metals Branch (RXLMN)
Metals, Ceramics and NDE Division
Materials and Manufacturing Directorate
Wright-Patterson Air Force Base, OH 45433-7750
Air Force Materiel Command, United States Air Force

Dayton Research Institute
Dayton, OH

The University of Texas
Austin, TX

8. PERFORMING ORGANIZATION REPORT NUMBER
AFRL-RX-WP-TP-2009-4162

9. SPONSORING/MONITORING AGENCY NAME(S) AND ADDRESS(ES)
Air Force Research Laboratory
Materials and Manufacturing Directorate
Wright-Patterson Air Force Base, OH 45433-7750
Air Force Materiel Command
United States Air Force

10. SPONSORING/MONITORING AGENCY ACRONYM(S)
AFRL/RXLMN

11. SPONSORING/MONITORING AGENCY REPORT NUMBER(S)
AFRL-RX-WP-TP-2009-4162

12. DISTRIBUTION/AVAILABILITY STATEMENT
Approved for public release; distribution unlimited.

13. SUPPLEMENTARY NOTES
To be submitted to Journal of ASTM International
PAO Case Number and clearance date: 88ABW-2008-0086, 16 January 2008.
The U.S. Government is joint author of this work and has the right to use, modify, reproduce, release, perform, display, or disclose the work.

14. ABSTRACT
The objective of this work was to evaluate life prediction methodologies involving fretting fatigue of turbine engine materials with advanced surface treatments. Fretting fatigue tests were performed on Ti-6Al-4V dovetail specimens with and without advanced surface treatments. These tests were representative of the conditions found in a turbine engine blade to disk attachment. Laser shock processing and low plasticity burnishing have been shown to produce deep compressive residual stresses with relatively little cold work. Testing showed these advanced surface treatments improved fretting fatigue strength by approximately 50%. In addition to advanced surface treatments, several specimens were also coated with diamond like carbon applied through a non-line-of-sight process capable of coating small dovetail slots in an engine disk. Testing with this coating alone and combined with advanced surface treatments also significantly improved fretting fatigue strength due to a decreased coefficient of friction along with the compressive residual stresses.

15. SUBJECT TERMS
Fretting, fatigue, crack growth, surface treatments, residual stress

16. SECURITY CLASSIFICATION OF:			17. LIMITATION OF ABSTRACT:	18. NUMBER OF PAGES	19a. NAME OF RESPONSIBLE PERSON (Monitor)
a. REPORT	b. ABSTRACT	c. THIS PAGE			James M. Larsen
Unclassified	Unclassified	Unclassified	SAR	32	19b. TELEPHONE NUMBER *(Include Area Code)* N/A

Standard Form 298 (Rev. 8-98)
Prescribed by ANSI Std. Z39-18

Influence of Residual Stresses on Fretting Fatigue Life Prediction in Ti-6Al-4V

Patrick J. Golden

Materials and Manufacturing Directorate, Air Force Research Laboratory, Wright-Patterson AFB, OH, USA

Dennis Buchanan

Structural Integrity Division, University of Dayton Research Institute, Dayton, OH, USA

Sam Naboulsi

The Institute for Computational Engineering and Sciences, The University of Texas, Austin, TX, USA

ABSTRACT

The objective of this work was to evaluate life prediction methodologies involving fretting fatigue of turbine engine materials with advanced surface treatments. Fretting fatigue tests were performed on Ti-6Al-4V dovetail specimens with and without advanced surface treatments. These tests were representative of the conditions found in a turbine engine blade to disk attachment. Laser shock processing and low plasticity burnishing have been shown to produce deep compressive residual stresses with relatively little cold work. Testing showed these advanced surface treatments improved fretting fatigue strength by approximately 50%. In addition to advanced surface treatments, several specimens were also coated with diamond like carbon applied through a non-line-of-sight process capable of coating small dovetail slots in an engine disk. Testing with this coating alone and combined with advanced surface treatments also significantly improved fretting fatigue strength due to a decreased coefficient of friction along with the compressive residual stresses. This work presents a mechanics based lifing

analysis of these tests that takes into account the local plasticity and the redistribution of residual stresses due to the contact loading. The use of superposition of the residual stresses into the contact stress analysis results in unconservative crack growth life predictions. Finite element analyses were conducted to predict the redistribution of residual stresses due to the contact loading. The redistributed residual stresses were used to make improved crack growth life predictions when possible. The results showed very little redistribution of residual stresses for the advanced surface treatments, however, a significant change in shot peened residual stress gradients was predicted.

KEYWORDS

Fretting; Fatigue; Crack Growth; Surface Treatments; Residual Stress

INTRODUCTION

Fretting occurs in many aerospace components such as the dovetail attachments of turbine blades and disks in turbofan engines or lap joints in aircraft structures. Designers often seek palliatives such as coatings or shot-peening to reduce the negative effects of fretting on the life of a component. Typically, however, the positive effect of these palliatives is not taken into account in the design life of a component. Instead it may be treated as an additional margin of safety. As the retirement age of aerospace vehicles continues to grow, the expected maintenance cost and burden also continues to increase. This drives the need for new palliatives and/or design methods that may allow safe increases in component usage before repair or replacement. One option is advanced surface treatments such as laser shock processing or low plasticity burnishing. These methods of inducing a layer of compressive residual stresses on a component,

although more costly than shot-peening, may allow new methods to take credit for residual stresses in design as proposed by Prevey and Jayaraman [1].

In order to take design credit for a process such as LSP or LPB it must be satisfactorily shown that the compressive residual stresses are sufficiently retained throughout the life of the component. Thermal relaxation, plastic deformation, or other sources of damage such as fretting or foreign object damage (FOD) could all potentially reduce or even reverse the effects of the compressive residual stresses. It is known that plasticity in fretting contacts plays an important role in the understanding of crack nucleation and propagation of cracks. Waterhouse [2] observed that many anti-fretting palliatives may be disrupted by plastic deformations. Plastic deformation in the substrate of a coated material, for example, may result in a loss of coating adhesion and effectiveness. Intentionally induced compressive residual stresses by methods such as shot-peening could also be disrupted by this plasticity.

Researchers have also proposed that the loss of residual stresses in a fretted material may be an indicator to fatigue damage [3]. The authors tested shot-peened fretting samples and made an array of residual stress measurements on the surface across the fretting scar. The results showed that the compressive residual stresses relaxed in the fretted region. It appears that this may be a different mechanism than the local plastic zone being proposed in this work since the relaxation appears over a wide region. Here, the accumulation of damage at the material surface (microcracking, scarring, etc.) may be responsible for the relaxation of residual stresses throughout the fretted region. Since only surface measurements were taken, it is not clear if this was only a surface phenomenon or if relaxation extended into the depth.

Previous work by the current authors applied mechanics based life prediction methods to a series of fretting fatigue tests that included coated specimens and specimens treated with LSP or

LPB [4]. The conclusion of this work was that mechanics based predictions were accurate and conservative for bare Ti-6Al-4V specimens and also for coated specimens. The analysis methods, however, over predicted the lives of LSP and LPB treated specimens. The objective of this paper was to investigate the redistribution of compressive residual stresses from several surface treatments due to plastic deformations in a fretting problem. The influence of different levels of compressive residual stress retention was also studied. The approach was to conduct elastic-plastic contact finite element method (FEM) analyses to determine the level of plasticity and residual stress redistribution in the fretting experiments.

EXPERIMENTS

The material used in this study was a Ti-6Al-4V alloy from the US Air Force National High Cycle Fatigue program [5]. The material was $\alpha + \beta$ forged then solution treated and overaged (STOA) at 932°C for 75 minutes, fan cooled, and mill annealed at 704°C for two hours. The resulting microstructure was approximately 60% primary α and 40% transformed β microstructure. All of the test specimens were machined from this material. The elastic modulus was 116 GPa and the 0.2% offset yield stress was 930 MPa. The ultimate tensile strength was 980 MPa. Monotonic and cyclic stress-strain curve fits were generated for this material and are plotted in Figure 1. The cyclic stress-strain curve were fit to the stress-strain hysteresis loops from multiple strain controlled low cycle fatigue tests measured at the half life of the specimens. These stress-strain curves will be used in the elastic-plastic contact models described later.

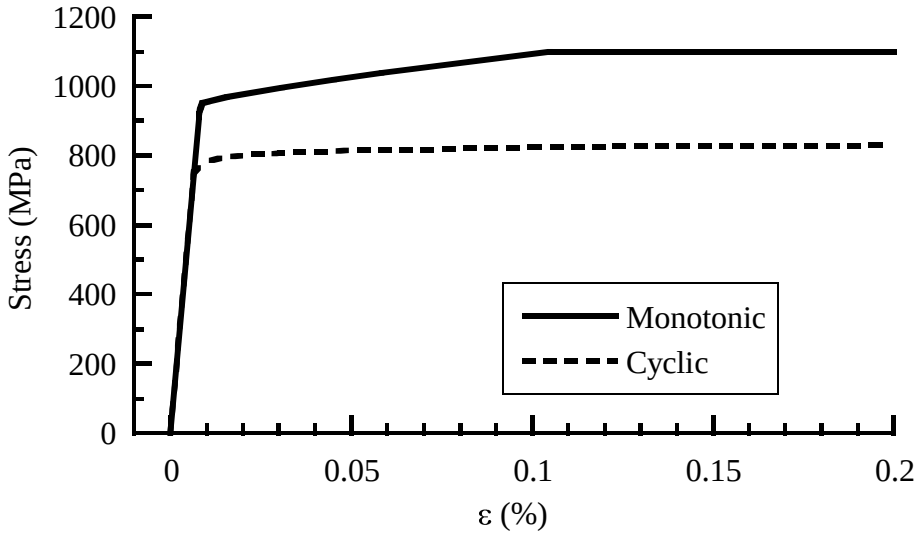

Figure 1: Monotonic and cyclic stress versus plastic strain curves used in the finite element analysis.

A photograph of the dovetail fretting experimental setup is shown in Figure 2. Development and testing with this fixture has been discussed previously by Conner and Nicholas [6] and Golden and Nicholas [7]. The steel fixture worked by pulling together a dovetail shaped test specimen and two fretting pads that had precisely machined surface profiles. Several surface profiles have been tested including cylindrical and flat with rounded edges with varying dimensions. All of the testing in this work were machined to a flat with rounded edges profile with a 3 mm flat and 3 mm radii. There were several key features to this setup that differ it from other fretting fatigue apparatus. First, the specimen was dovetail shaped which resulted in cyclic loading of both the normal, *P*, and shear, *Q*, contact forces rather than only cyclic applied *Q*. Second, the fixture was designed with replaceable fretting pads. Each experiment only required replacement of the pads rather than the entire fixture as with other dovetail fatigue experiments [8]. Finally, it was not possible to obtain direct measurement of the contact forces *P* and *Q*.

Many other fretting fatigue test setups did allow direct measurement of the contact forces through placement of load cells in the load path [9]. Instrumentation of the contact loads, however, was critical to allow validation of life prediction methods. Instrumentation was achieved through the addition of strain gages to the fxture in location of peak strain. Calibration of the contact forces to the strain gages was achieved through finite element modeling of the fixture as discussed in Golden and Nicholas [7].

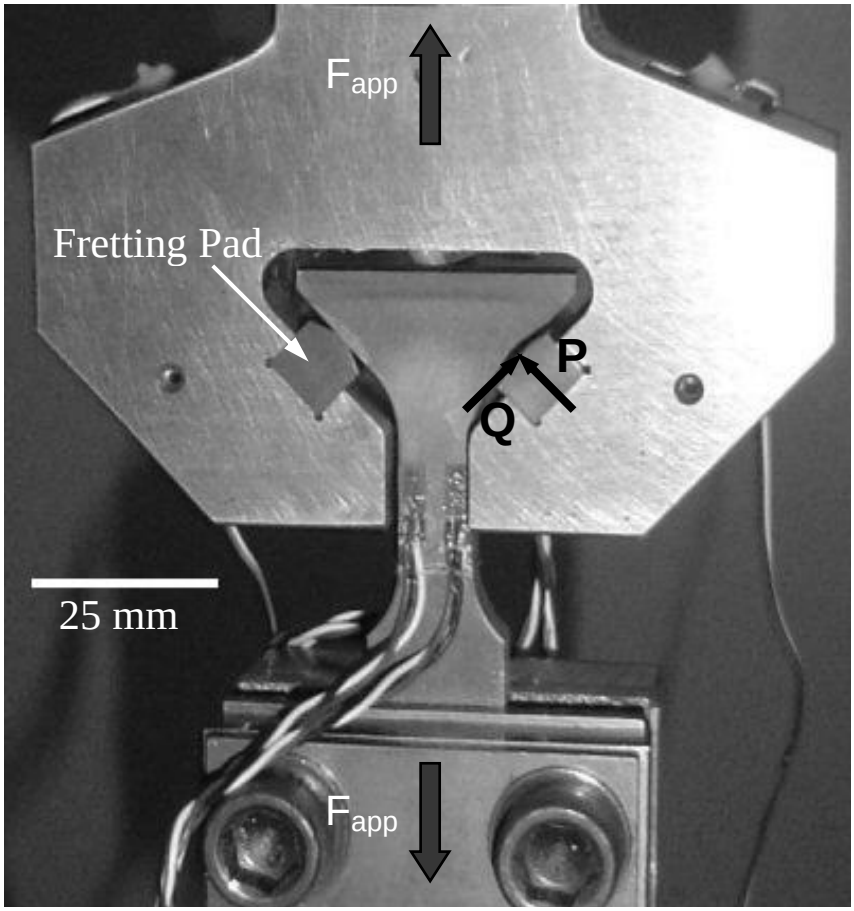

Figure 2: Photograph of the dovetail fretting fatigue setup.

The focus of this effort was to test and model the effects of coatings and residual stress surface treatments on dovetail fretting. Laser shock processing (LSP) and low plasticity

burnishing (LPB) were each applied to six specimens in the regions of contact. Half of these and an additional five untreated specimen were also coated with diamond like carbon (DLC). Several specimens were sent post-test for destructive measurement of the in-depth residual stresses. The measurements were made using x-ray diffraction in a region of the specimens just outside of the fretting scars. In-depth measurements were made by layer removal with electropolishing. The results were shown previously in Golden et al. [11] and curve fits of those results have been plotted in Figure 3. Also plotted is a typical residual stress profile of a shot-peened Ti-6Al-4V specimen peened with steel shot at 6-8A intensity. These profiles were used in the stress analysis and life prediction described later. Note that the shot-peening profile has a significantly higher magnitude than both the LSP or LPB profiles, but the LSP and LPB processes provide a much deeper layer of compressive residual stress.

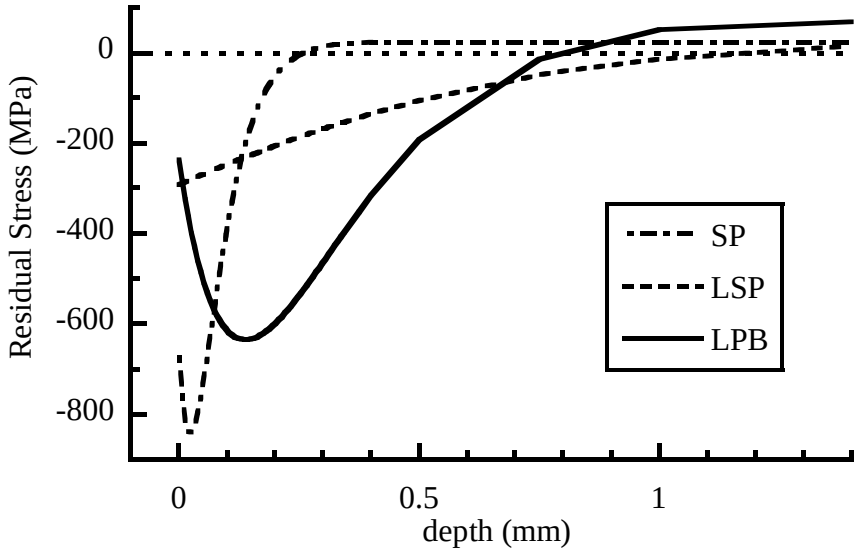

Figure 3: Residual stress profile curve fits. The LSP and LPB curves were fit to measurements made in this work. The SP curve is fit to typical 6-8A intensity peening data on Ti-6Al-4V.

Room temperature tests at a load ratio $R = 0.1$ were conducted at several load levels on bare Ti-6Al-4V, LSP treated, LPB treated, DLC coated, LSP + DLC, and LPB + DLC. The results were plotted in Figure 4 and have been described previously in Golden et al. [11]. Both the residual stress treated specimens and the DLC treated specimens each extend the life by an order of magnitude. When DLC was combined with LSP or LPB none of the specimens were able to be failed. The fatigue load limit of the fixture was exceeded before failure of the specimens could occur. The contact loads and average friction coefficients for each of these tests were measured and will be used in the stress analysis and life prediction described below.

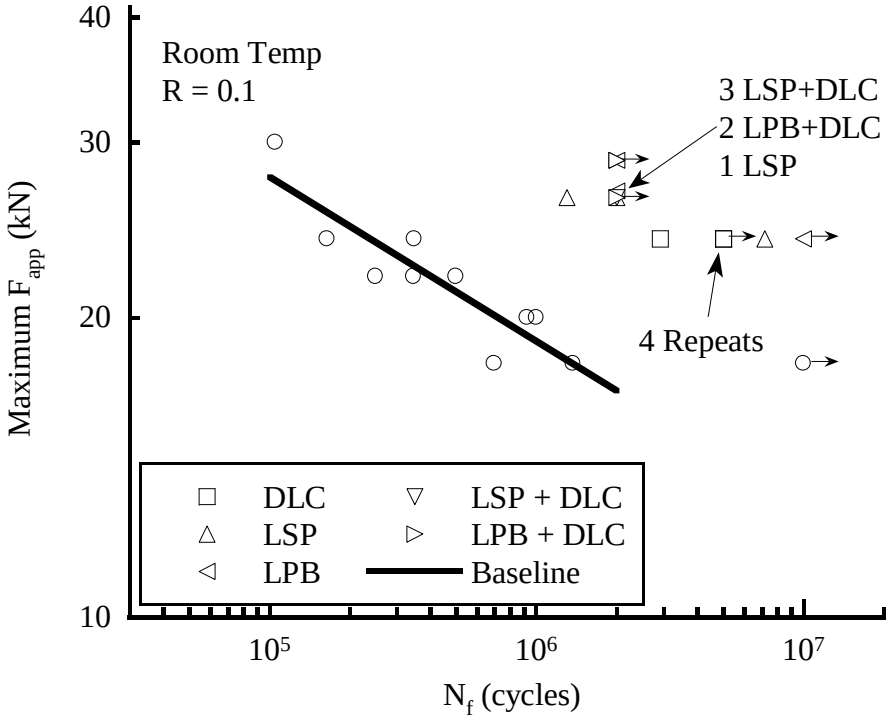

Figure 4: Results of the dovetail fretting fatigue tests with advanced surface treatments and diamond like carbon coating.

ANALYTICAL PROCEDURES

Several different analysis procedures have been applied in this work. The overall objective of this research was to develop and demonstrate effective deterministic analysis methods that will allow accurate life prediction in dovetail geometry. These methods accounted for changes in friction and residual stress due to surface treatments and processing. The mechanics based approach taken was dependent on the quality of the contact force measurement or prediction as well as the stress analysis tools. In this study, the contact forces were determined experimentally as discussed above. In general, however, the contact forces and the bulk stresses would be predicted from the results of a global FEM model. In either case, the local contact stresses were then calculated using the contact geometry and forces as input to a singular integral equation (SIE) solution (described below). In the case of applied surface treatments and/or local plasticity the residual stresses must be superimposed with the applied stresses. The effects of redistribution of residual stresses were a focus of the elastic-plastic contact modeling conducted in this work. Once a complete stress field has been calculated, standard nucleation and fracture mechanics life prediction methods were applied.

Figure 5 shows two schematics that represent the contact in the current experimental setup and the equivalent geometry used in the contact mechanics analysis. In the experiment, the dovetail specimen was pulled down into the contact pad. The contact pad had a surface profile that was described by $h(x)$. In this case, the profile was a 3 mm flat with 3 mm radii at the edges of contact. In general, the configuration could have two materials; the specimen (E_1, ν_1) and the pad (E_2, ν_2), but in this study the materials were both Ti-6Al-4V. Although the contact forces were known from the experiment, the bulk stresses in the contact region were not. Prior studies [12,13] have described a method to extract the bulk stress from the FEM analysis in the contact

region of a dovetail configuration. In short, the bulk stress was the FEM stress solution minus the contact stresses. Once the contact stresses were determined analytically as described below, they were subtracted from the FEM stress results to obtain the bulk stress. The reason an FEM and an SIE analytical solution were both used was that each had an advantage and a disadvantage in terms of accuracy and efficiency. The FEM solution accounted for all of the specimen or component geometric features, whereas the SIE solution did not. The SIE solution was very fast and accurate at obtaining the very steep edge of contact stress gradient, whereas the FEM solution had long computational times and it was often not possible to obtain a converged stress solution at the edge of contact, particularly in 3-D models.

The second schematic in Figure 5 shows the configuration used in the SIE analysis. A Matlab script named CAPRI was used to solve the singular integral equations (SIE) that describes the contact between two similar materials with a gap function *h(x)*. CAPRI was written at Purdue University to calculate the normal and shear contact tractions and the subsurface stresses for an arbitrary indenter that is pressed into a semi-infinite body [14]. The influence of the bulk stress plays a role in the calculation of the contact tractions, but must be a known input and is not an output of the analysis. Thus, there is often a need for an FEM analysis to determine the bulk stress as described above. Once the SIE contact stress analysis including the bulk stress is complete, stress gradients can be extracted along the expected crack growth paths as shown in Figure 5.

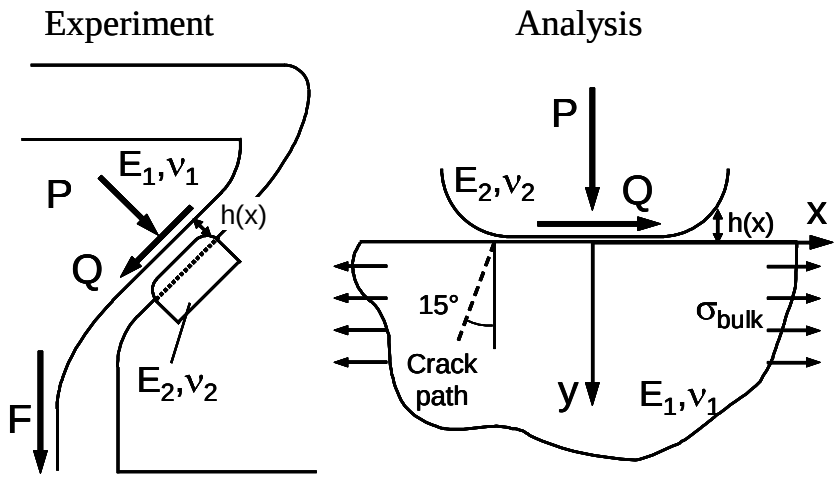

Figure 5: Schematic of an equivalent geometric representation of an actual dovetail used in the singular integral equation solution to the contact problem.

After the stress gradients were calculated the next step was to calculate nucleation and fracture mechanics stress intensity factor, *K*. Nucleation was not the focus of this effort; however, prior work [15] had used an equivalent stress methodology to calculate nucleation life based on surface stresses. This model includes the multi-axial components of stress and used a stressed area approach to account for the local stress peak at the edge of contact. *K* solutions were calculated using the weight function methodology. Mode I surface crack and through crack weight function *K* solutions were written in Matlab to efficiently work with the output of CAPRI [12,16,17]. Negative K_I values were allowed to be calculated in the case of the residual stress gradients and were plotted in Figure 6. Superposition of the residual stress K_I with the maximum and minimum applied K_I resulted in a total ΔK_I that had a shift in *R*. An effective stress intensity factor range, ΔK_{eff}, was then used to account for this changing *R* as calculated in Equation 1. Figure 7 is a plot of ΔK_{eff} versus crack size. Here, *m* is an exponent fit from crack growth data at *R* values of -1, 0.1, 0.5, and 0.8 [5] and equals 0.72 for positive *R* and 0.275 for negative *R*. The

crack growth rate and propagation life was then calculated from ΔK_{eff} using the sigmoidal crack growth law shown in Equation 2. Here B, P, Q, d, K_{th}, and K_c were constants fit to the crack growth data with values of -18.1, 3.71, 0.235, -0.0066, 4.21 $MPa\sqrt{m}$, and 66 $MPa\sqrt{m}$ respectively. The crack growth rate da/dN data were in units of m/cycle.

$$\Delta K_{eff} = K_{\max} \left(1 - R\right)^{m} \tag{1}$$

$$\frac{da}{dN} = 0.0254 \times e^{B}\left(\frac{\Delta K_{eff}}{K_{th}}\right)^{P}\left[\ln\left(\frac{\Delta K_{eff}}{K_{th}}\right)\right]^{Q}\left[\ln\left(\frac{K_c}{\Delta K_{eff}}\right)\right]^{d} \tag{2}$$

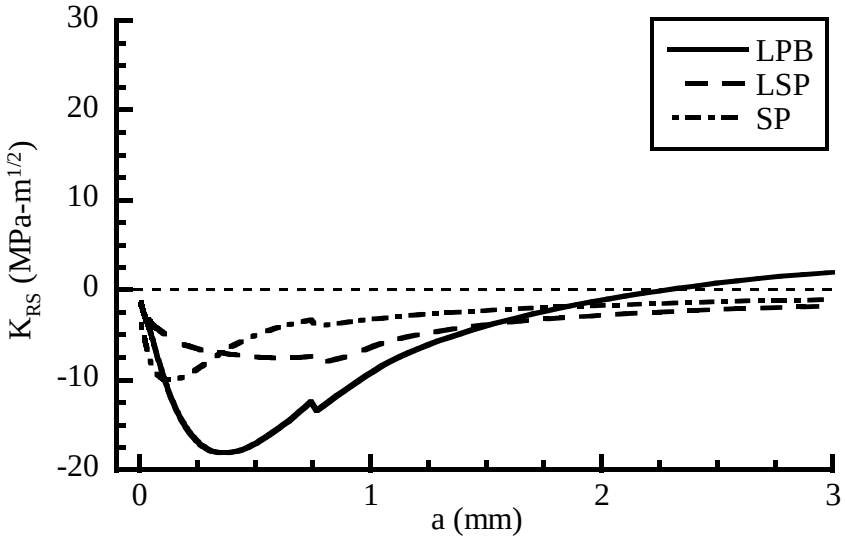

Figure 6: Stress intensity factor due to residual stress gradients.

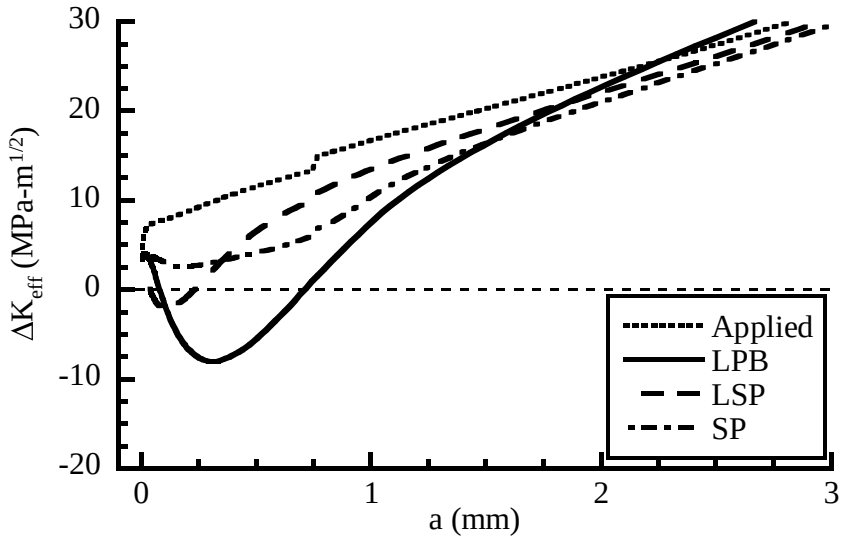

Figure 7: Stress intensity factor range for combined applied load and residual stress.

A finite element model was generated to represent the dovetail fretting fatigue experiment loading conditions and is shown in Figure 8. A simplified geometry of a 2-D plate and contact pad was chosen rather than modeling the actual dovetail geometry. The maximum and minimum contact forces, *P*, *Q*, and *M*, from the experiments were applied to the top surface of the contact pad in a cyclic manner. Five load cycles were found to be sufficient to stabilize the elastic-plastic response. Constraints were applied to the fretting pad to distribute the applied loads and to control its rotation. The bulk stress was applied to the end of the plate, which represented the fretting specimen. The plate was 15 mm deep by 60 mm long and had roller constraints on the edges opposite the contact and bulk stress as shown in Figure 8. The model was analyzed in ABAQUS and was meshed with 2-D plane strain 4-node bilinear elements. The element size in the contact region was 5 μm by 5 μm which was sufficient to capture the very high stress peaks at the edge of contact and the plastic zone that developed. The nonlinear combined isotropic/kinematic model provided in ABAQUS was used. The cyclic and monotonic stress

strain curves plotted in Figure 1 were the only data available for this analysis. The model was run using both sets of data with very little difference in results for these problems. The results shown in the following section were analyzed using the cyclic stress-strain curve.

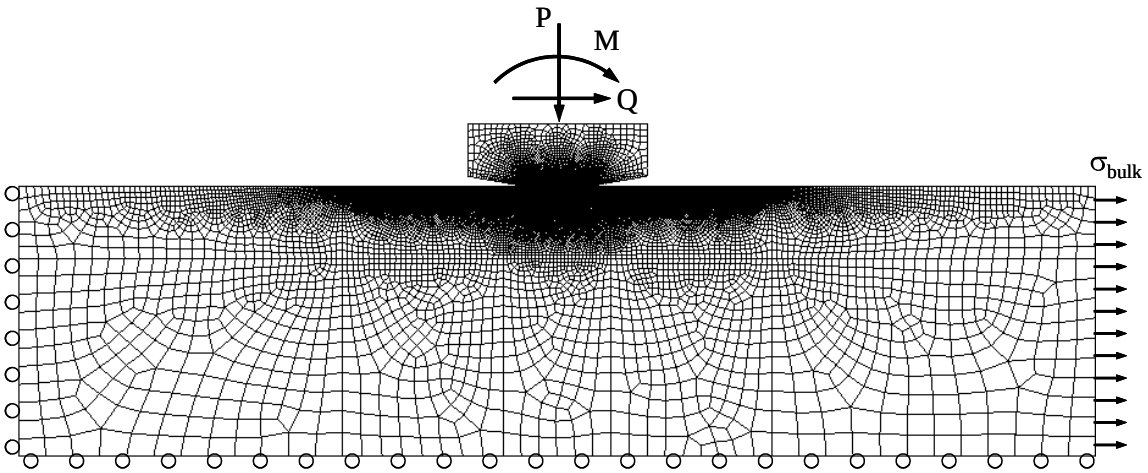

Figure 8: Finite element model used to represent the loading conditions in the dovetail fretting tests.

RESULTS AND DISCUSSION

The results of this work consist of the output of the elastic-plastic contact finite element analysis, changes in the residual stress profiles, and the resulting influence on life predictions. The life predictions in this work are focused entirely on crack propagation including short crack growth, rather than nucleation plus propagation. Prior work [18] has shown that at the end of interrupted fretting fatigue tests in Ti-6Al-4V cracks were often found very early in the expected life of the specimens. Also, nucleation life predictions on these experiments [12] have previously been shown to be on the order of 10% of the total life or less. This was expected

since the stresses at the edge of contact were typically well above yield in an elastic analysis, and then rapidly decreased. This lead to early crack nucleation followed by relatively slow early crack growth. Additionally, all of the analysis in this work was limited to mode I fracture mechanics. Again, previous analysis on these experiments [12] as well as on other fretting fatigue experiments [19] have shown that any mode II contribution to crack growth was expected to be quite small. Although the calculated value of K_{II} was significant, ΔK_{II} was not. This, however, did not imply that all cracks grew perpendicular to the surface. In fact, the experiments showed that the macroscopic cracks grew approximately 15-25° from normal in a direction away from the center of contact. This was accounted for in the fracture mechanics calculations.

In these experiments, many of the treated specimens ended as run-outs and did not fail. It was predicted from the stress analysis, nucleation model, and fracture mechanics that despite the compressive residual stresses and/or the low friction coatings that cracks would still form at the edge of contact and grow a short length before arresting. This, in fact was the case as demonstrated in Figure 9. Figure 9 is an SEM micrograph showing a crack that grew from the edge of contact in a specimen treated with LPB. The section was mounted, ground, and polished in the specimen thickness direction. The crack was nearly 100 μm deep in this cross-section which was near the maximum depth found for this crack. The fracture mechanics analysis with the El Haddad short crack correction [20] for this specimen predicts crack arrest at a depth of approximately 60 μm when the full residual stress gradient is superimposed with the applied stress gradient. The actual crack length is longer than the predicted crack arrest which is generally consistent with the unconservative fracture mechanics life predictions for these experiments that was discussed earlier. The observation of a crack in this and other run-out specimens did, however, validate the analytical results that showed cracks can nucleate, grow,

and arrest under fretting fatigue. This has been observed in run-out tests with and without residual stresses due to LSP or LPB.

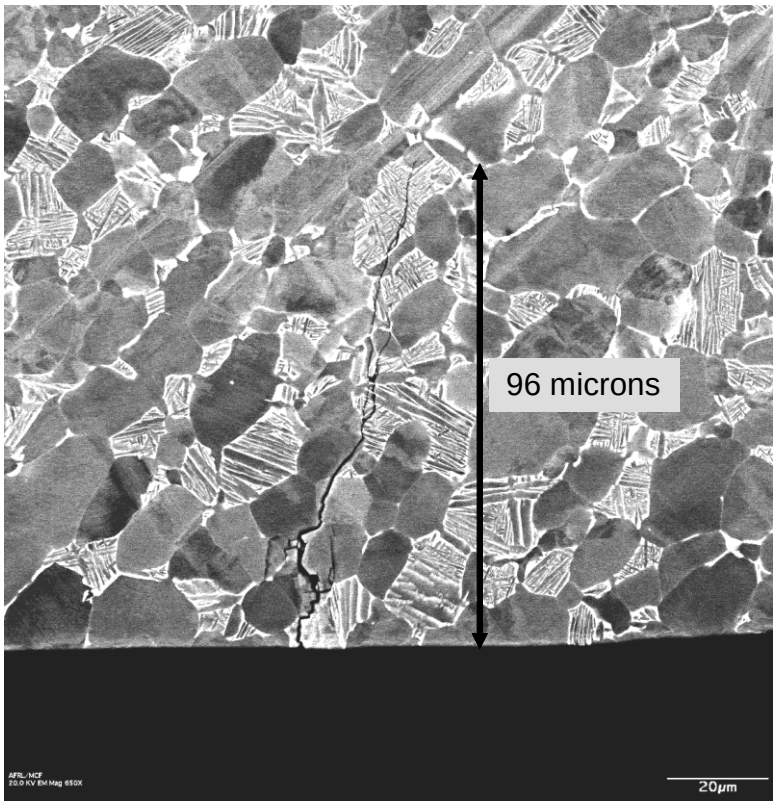

Figure 9: Profile of a crack located at the edge of contact found post-test in a run-out experiment that had been processed with LPB.

The contact finite element analysis with plasticity and initial residual stress distribution was conducted for the LSP, LPB, and SP conditions. Several different loading conditions were analyzed. These load cases used minimum and maximum values of *P*, *Q*, *M*, and bulk stress taken directly from the experiments. They were representative of the range from the least to most severe load cases found in the actual experiments. Multiple steps of maximum and minimum load were run until the plastic zone stabilized. Five cycles was found to be sufficient.

Analyses with both the cyclic and the monotonic stress-strain curves were run and compared, but since the plasticity was so localized the difference was very small. The final result of interest was the change in the initial residual stress in the model, so the final load step in the analysis was unloading to zero applied loads. Figure 10 is an example of redistributed shot-peen residual stresses in the specimen. The fretting pad is not shown. The surface to the right of the crack location is under the contact. The component of stress shown is the normal stress parallel to the surface. The affected zone was an approximately 300x300 μm area at the edge of contact. It is observed that a significant amount of redistribution was predicted to occur in this very small volume. This could significantly affect crack growth predictions for shot peened specimens in the short crack regime. A plot of the redistributed SP residual stress is shown in Figure 11a. This stress was taken along a path from the edge of contact into the depth and was compared to the original SP residual stress gradient. The distribution peak was significantly pushed into the tensile direction for the first 70 μm. This result is important, because this peak is what is responsible for leading to potential early crack arrest and providing a fatigue benefit. Figure 11b, however, shows that for the LPB treated specimens a very different redistribution of the residual stress gradient occurred. The LSP treated specimens had a nearly identical trend. Here, the near surface stresses were pushed more compressive. Slightly deeper, the residual stress becomes more tensile to compensate.

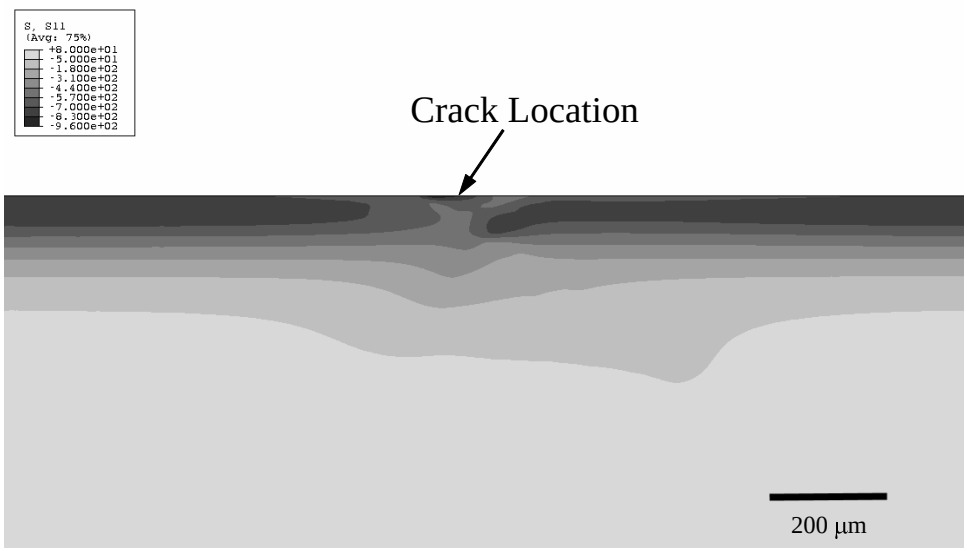

Figure 10: Contours of shot-peen residual stress, σ_{xx}, at the edge of contact after stress redistribution. Contours range from +80 (light) to -960 MPa (dark) in 130 MPa increments.

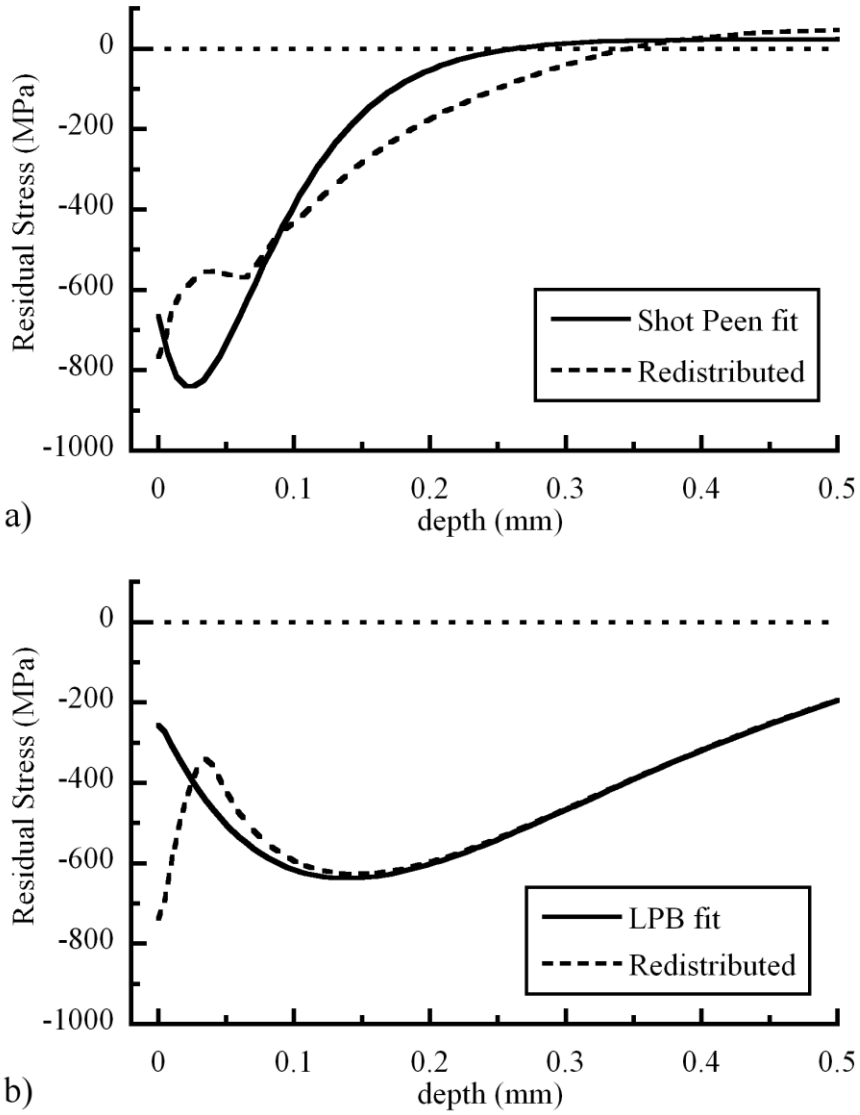

Figure 11: Predicted redistribution of residual stress at the edge of contact for typical contact loading case for both a) shot peening and b) LPB.

The mechanisms for the different results in SP and LSP or LPB specimens can be explained as followed. The modeling showed that the high compressive stress due to contact during the negative shear reversal can combine with the compressive residual stresses to result in a localized plastic zone as was hypothesized. This was seen in the finite element results shown in Figures 10 and 11a. The compressive yield results in a region of residual stresses that are

shifted in the tensile direction. At the very near surface (20 microns deep) tensile yield occurs in the shot peened example (Figure 11a) due to the high tensile stress due to contact during the positive shear reversal. This results in more compressive residual stresses at the surface (0-5 μm). The compressive yield zone was larger (60-70 microns deep) than the tensile, however, so there is a zone of more tensile residual stress (5-70 μm) . Beyond 70 μm the residual stresses become more compressive to compensate. In the LPB treated samples, it yielding was not predicted to occur during the negative shear reversal. This was because the highest compressive stresses due to the applied loading occur very near the surface, while the highest compressive residual stresses occur deeper in the subsurface than those due to shot peening. The two compressive stress peaks (applied and residual) did not sufficiently overlap to result in a predicted plastic zone in the case of LPB. This was reflected in the predicted redistribution shown in Figure 11b. Here, the redistribution was due entirely to the tensile yield that occurs at the surface in the edge of contact during the positive shear reversal. The compressive residual stresses due to LPB were smaller near the surface than those due to shot peening which also resulted in a larger predicted tensile plastic zone. Residual stress measurements of the specimens at the edge of contact were never performed. It was believed by the authors that the minimum x-ray spot sizes available using the x-ray diffraction technique were much too large to capture any expected localized change in residual stress. This may be an area of future work to either help confirm the analysis results or better explain the experimental results.

These predictions were based entirely on homogeneous material properties. The predicted plastic zone depths, however, were on the order of only a few grains. The local microstructure was not taken into account in the analysis. Goh, et al. [21] showed that crystal plasticity may result in quite different results in predictions of localized plastic zones. In their simulations of

plasticity under a fretting contact they showed that in the case of homogeneous material properties a small zone of cyclic plasticity develops surrounded by a larger zone that reaches an elastic shakedown condition. Much like the results predicted in this work. When the same material was modeled with crystal plasticity, however, a much deeper zone of ratcheting and cyclic plasticity was predicted. Although this type of analysis has not been conducted for the experiments in this work, Goh's results suggests that a more accurate analysis using crystal plasticity could result in a larger and deeper influence on residual stress redistribution.

The results of this work lead to the questions of how much of a reduction in the residual stress gradient is required to lead to life predictions that match the experimental results. Is a redistribution of residual stresses alone enough to explain the unconservative life predictions, or are some other sources of uncertainty in the analysis more important? To help answer these questions the life prediction analyses were repeated with different levels of residual stress gradients. The SP, LSP, and LPB gradients were each scaled to 100%, 80%, 50%, 35%, 20%, and 0% and the analyses were repeated for all of the respective fretting experiments. The SP gradients were applied to the uncoated LSP and LPB experiments for comparison since there were no shot peened experiments to analyze. An example of the results of this analysis is shown in Figure 12. Crack growth to failure was predicted from a range of initial flaw sizes. In this example, 50% of the LPB residual stress gradient or higher was predicted to result in no crack growth for crack lengths smaller than approximately 0.5 mm. Smaller crack lengths were either below the crack propagation threshold or not predicted to have positive stress intensity factors. Approximately 35% of the LPB residual stress gradient resulted in a finite life prediction of approximately 2 million cycles. Since the actual specimen was a 10 million cycle run-out, the predicted remaining level of residual stresses in the specimen was between 35% and 50%. A

similar analysis was conducted on all of the LSP and LPB experiments and also the hypothetical SP samples. The predicted remaining level of residual stresses in the LSP specimens was 50-80%. The predicted remaining level of residual stresses in the SP specimens that would result in some specimens failing was 35-50%.

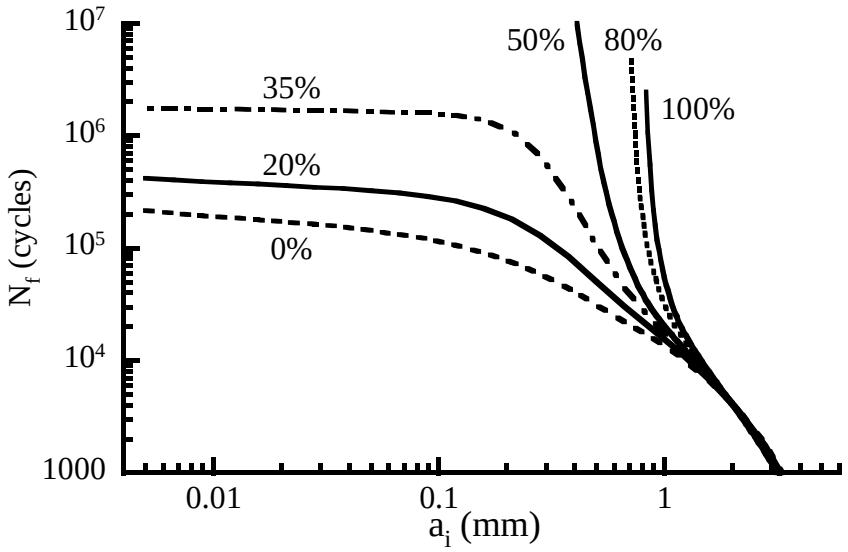

Figure 12: Predicted remaining life as a function of crack length and percent retained residual stress due to LPB for a typical fretting experiment.

One additional observation from these analyses has been that the SP residual stress gradient could be predicted to be just as effective at preventing growth of fretting fatigue cracks as the LSP or LPB residual stress gradients. Even though the LPB gradient was much deeper than the SP gradient, it appeared that the magnitude and depth of the SP gradient sufficient to prevent cracks of significant length (0.3 mm) from growing in these experiments, if the original residual stresses remain unaltered. What the elastic-plastic contact analysis in this work showed, however, was that the SP residual stress gradients appeared to be more easily altered due to

redistribution from local plasticity than the LSP or LPB residual stresses. Additionally, prior research showed that shot peened Ti-6Al-4V was more susceptible to thermal relaxation than either LSP or LPB [22]. This was explained as being a result of the much higher level of cold work imparted on the material in shot peening than in LSP or LPB. A thorough understanding of the loading and thermal conditions and the possibility of tensile or compressive local yielding are thus important factors to consider when designing a fatigue critical location with SP, LSP, or LPB.

CONCLUSIONS

Mechanics based life predictions of LSP and LPB treated fretting fatigue experiments resulted in unconservative life predictions. An elastic-plastic contact analysis was conducted to determine the influence of plastic deformations on the residual stresses. The compressive stress from the applied loading at the edge of contact during the reverse shear cycle was predicted to be elastic under the test conditions in these experiments. When the applied compression was combined with shot-peening compressive residual stresses, however, a compressive yield zone formed that redistributed the compressive residual stresses in the tensile direction. This compressive yield zone did not form in the case of LSP or LPB treated samples, because the peak compression was either deeper in the material or because the peak magnitude of compression was smaller than for shot-peening. Based on the results of the finite element modeling, it could be concluded that redistribution of the residual stresses due to plasticity was not the source of the unconservative life predictions on these experiments.

The elastic-plastic contact analysis of shot-peened specimens showed a significant redistribution of the residual stresses. Although no experiments were conducted with shot-

peening in this work, this result reaffirms the current practice of not taking credit for shot peening residual stresses in design.

Life predictions were conducted on all of the fretting experiments with different levels of retained residual stresses. Predictions were then made to determine the level of retained residual stresses that would make the predicted lives match the actual fretting fatigue lives. The required level of retained residual stresses in the LPB specimens to correlate with the experiments was 35-50%. In the LSP specimens, the level of retained residual stresses that best correlated with the experiments was 50-80%. This lead the authors to believe that other sources of uncertainty besides the residual stresses not considered in the current deterministic analysis may be driving the unconservative life prediction results.

REFERENCES

[1] Prevey P, Jayaraman J, "A Design Methodology to Take Credit for Residual Stresses in Fatigue Limited Designs," Journal of ASTM International, 2, n 8, Sep 2005.

[2] Waterhouse RB, "Plastic Deformation in Fretting Processes – a Review," Fretting Fatigue: Current Technology and Practices, ASTM STP 1367, DW Hoeppner, V Chandrasekaran, and CB Elliott, Eds., American Society of Testing and Materials, West Conshohocken, PA, 2000.

[3] Martinez SA, Sathish S, Blodgett MP, Mall S, Namjoshi S, "Effects of Fretting Fatigue on the Residual Stress of Shot Peened Ti-6Al-4V Samples," Mat. Sci. Eng. A, 399, 2005, pp. 58-63.

[4] Golden PJ, Shepard MJ, "Life Prediction of Fretting Fatigue with Advanced Surface Treatments," Materials Science and Engineering: A, doi:10.1016/j.msea.2006.10.168, 2007.

[5] Gallagher JP, et al., AFRL-ML-TR-2001-4159, Improved High-Cycle Fatigue (HCF) Life Prediction, Wright-Patterson Air Force Base, OH, January 2001.

[6] Conner BP, Nicholas T, "Using a Dovetail Fixture to Study Fretting Fatigue and Fretting Palliatives," Journal of Engineering Materials and Technology, 128, 2006, pp. 133-141.

[7] Golden PJ, Nicholas T, "The Effect of Angle on Dovetail Fretting Experiments in Ti-6Al-4V," Fatigue and Fracture of Engineering Materials and Structures, 28, 2005, pp. 1169-1175.

[8] Ruiz C, Boddington PHB, Chen KC, "An Investigation of Fatigue and Fretting in a Dovetail Joint," Experimental Mechanics, 24, 1984, pp. 208-217.

[9] Hills DA, Nowell D, "Mechanics of Fretting Fatigue," Kluwer, London, 1994, pp. 153-168.

[10] McVeigh PA, Harish G, Farris TN, Szolwinski MP, "Modeling Interfacial Conditions in Nominally Flat Contacts for Application to Fretting Fatigue of Turbine Engine Components," International Journal of Fatigue, 21(S), 1999, pp. 157-165.

[11] Golden, P.J., Hutson, A.L., Sundaram, V., Arps, J.H., "Effect of Surface Treatment on Fretting Fatigue of Ti-6Al-4V," International Journal of Fatigue, 29, 2007, pp. 1302-1310.

[12] Golden PJ, Calcaterra JR, "A Fracture Mechanics Life Prediction Methodology Applied to Dovetail Fretting," Tribology International, 39, 2006, pp. 1172-1180.

[13] Rajasekaran R, Nowell D, "Fretting Fatigue in Dovetail Blad Roots: Experiments and Analysis," Tribology International, 39, 2006, pp. 1277-1285.

[14] Murthy, H., Harish, G., Farris, T.N., "Efficient Modeling of Fretting of Blade/Disk Contacts Including Load History Effects," Journal of Tribology, 126, 2004, pp. 56-64.

[15] Murthy H, Rajeev PT, Farris TN, Slavik DC, "Fretting Fatigue of Ti-6Al-4V Subjected to Blade / Disk Contact Loading," In: Developments in Fracture Mechanics for the New Century, 50th Anniversary of Japan Society of Materials Science, Osaka, Japan, 2001, pp. 41-48.

[16] Shen G, Glinka G, "Weight Functions for a Surface Semi-Elliptical Crack in a Finite Thickness Plate," Theoretical and Applied Fracture Mechanics, 15, 1991, pp. 247-255.

[17] Glinka G, Shen G, "Universal Features of Weight Function for Cracks in Mode I," Engineering Fracture Mechanics, 40, 1991, pp. 1135-1146.

[18] Hutson AL, Neslen C, Nicholas T, "Characterization of Fretting Fatigue Crack Initiation Processes in Ti-6Al-4V," Tribology International, 36, 2003, pp. 133-143.

[19] Nicholas T, Hutson A, John R, Olson S, "A Fracture Mechanics Methodology Assessment for Fretting Fatigue," International Journal of Fatigue, 25, 2003, pp. 1069-77.

[20] El Haddad MH, Smith KN, Topper TH, "Fatigue Crack Propagation of Short Cracks," Journal of Engineering Materials and Technology, 101, 1979, pp. 42-46.

[21] Goh CH, McDowell DL, Neu RW, "Plasticity in Polycrystalline Fretting Fatigue Contacts," Journal of the Mechanics and Physics of Solids, 54, 2006, pp. 340-367.

[22] Shepard MJ, Prevey PS, Jayaraman N, "Effects of Surface Treatment on Fretting Fatigue Performance of Ti-6Al-4V," 8th National High Cycle Fatigue Conference, 2003.